

² **Supplementary material for: Monte Carlo simulation**
³ **method of polarization effects in Laser Compton**
⁴ **Scattering on relativistic electrons**

⁵ **Dan Filipescu^a**

⁶ ^a*Horia Hulubei National Institute of Physics and Nuclear Engineering (IFIN-HH), 30 Reactorului, 077125
7 Bucharest, Romania*

⁸ *E-mail:* dan.filipescu@nipne.ro

⁹ **ABSTRACT:** Simulations for the interaction between:

- ¹⁰ • 1 nm/1.24 keV X-ray beam and 10 MeV electron beam;
- ¹¹ • 100 pm/12.4 keV X-ray beam and 10 MeV electron beam;
- ¹² • 50 pm/24.8 keV X-ray beam and 10 MeV electron beam;
- ¹³ • 10 pm/124 keV X-ray beam and 10 MeV electron beam;
- ¹⁴ • 532 nm/2.33 eV laser beam and 500 MeV electron beam;
- ¹⁵ • 532 nm/2.33 eV laser beam and 3500 MeV electron beam;

¹⁶ The angle of incidence was varied with 18° steps from head-on $\theta_i = 0^\circ$ up to $\theta_i = 162^\circ$. Ideal
¹⁷ electron and photon beams have been considered. For all cases, a linear polarized incident photon
¹⁸ beam was considered, with the plane of polarization situated in plane ($\tau = 0^\circ$) and perpendicular
¹⁹ ($\tau = 90^\circ$) to the plane defined by the incident photon and electron beams. The electron beam was
²⁰ considered to be unpolarized.

²¹ For high energy electron beams of 500 and 3500 MeV, the geometry for the NewSUBARU
²² BL01 was considered, with the interaction point placed in the center of the straight beam-line and
²³ the imaging plate was placed at 12 m downstream of it, in front of the C1 collimator position. For
²⁴ low energy electron beams of 10 MeV, the the imaging plate was placed at 1.5 m downstream of
²⁵ the interaction point.

²⁶ **KEYWORDS:** Only keywords from JINST's keywords list please

²⁷ **ARXIV EPRINT:** [1234.56789](https://arxiv.org/abs/1234.56789)

²⁸ **Contents**

²⁹ **1 Simulation results**

³⁰ The figures presented here show the simulation results related to the polarization properties in the
³¹ cases mentioned in the abstract. Each line corresponds to a given incident angle between incident
³² photon and electron beams. Starting from top to bottom, the results are represented for 0° (head-on),
³³ 18° , 36° , 54° , 72° , 90° , 108° , 126° , 144° and 162° . Starting from left to right, the odd columns
³⁴ correspond to incident photon linear polarization lying in the defined by the incident photon and
³⁵ electron beams ($\tau = 0^\circ$), while the even columns correspond to perpendicular polarization plane
³⁶ ($\tau = 90^\circ$).

³⁷ For each case, the figures show:

- ³⁸ • columns 1 and 2: γ -ray beam intensity spatial distribution on the imaging plate;
- ³⁹ • columns 3 and 4: $P_1^{(LAB)}$ Stokes parameter distribution as function of γ -ray energy;
- ⁴⁰ • columns 5 and 6: γ -ray energy distribution of polarization vector azimuthal angle;
- ⁴¹ • columns 7 and 8: $P_1^{(LAB)}$ spatial distribution on the imaging plate.

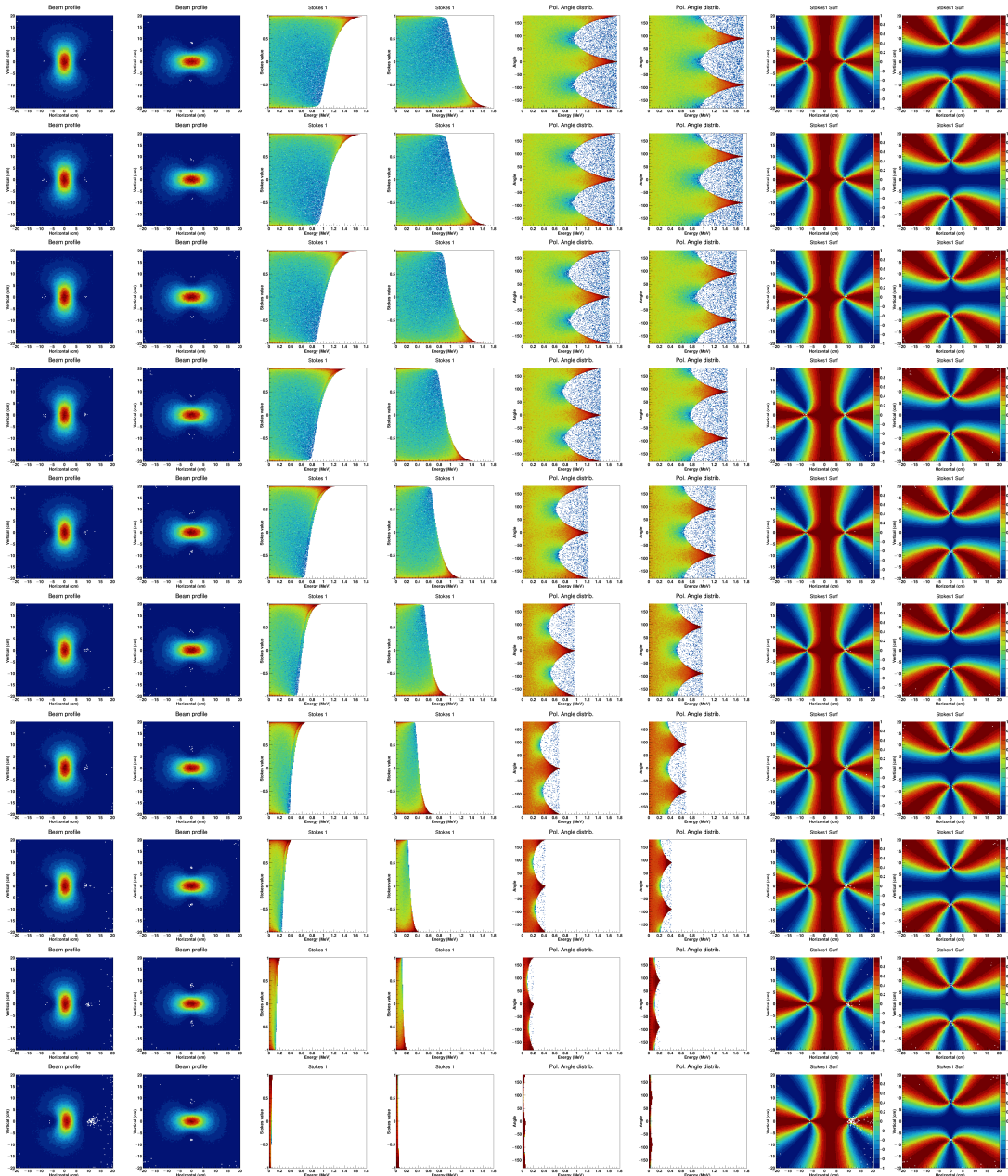


Figure 1. Compton scattering of 100 % linear polarized 1000 pm wavelength X-rays on 10 MeV electrons.

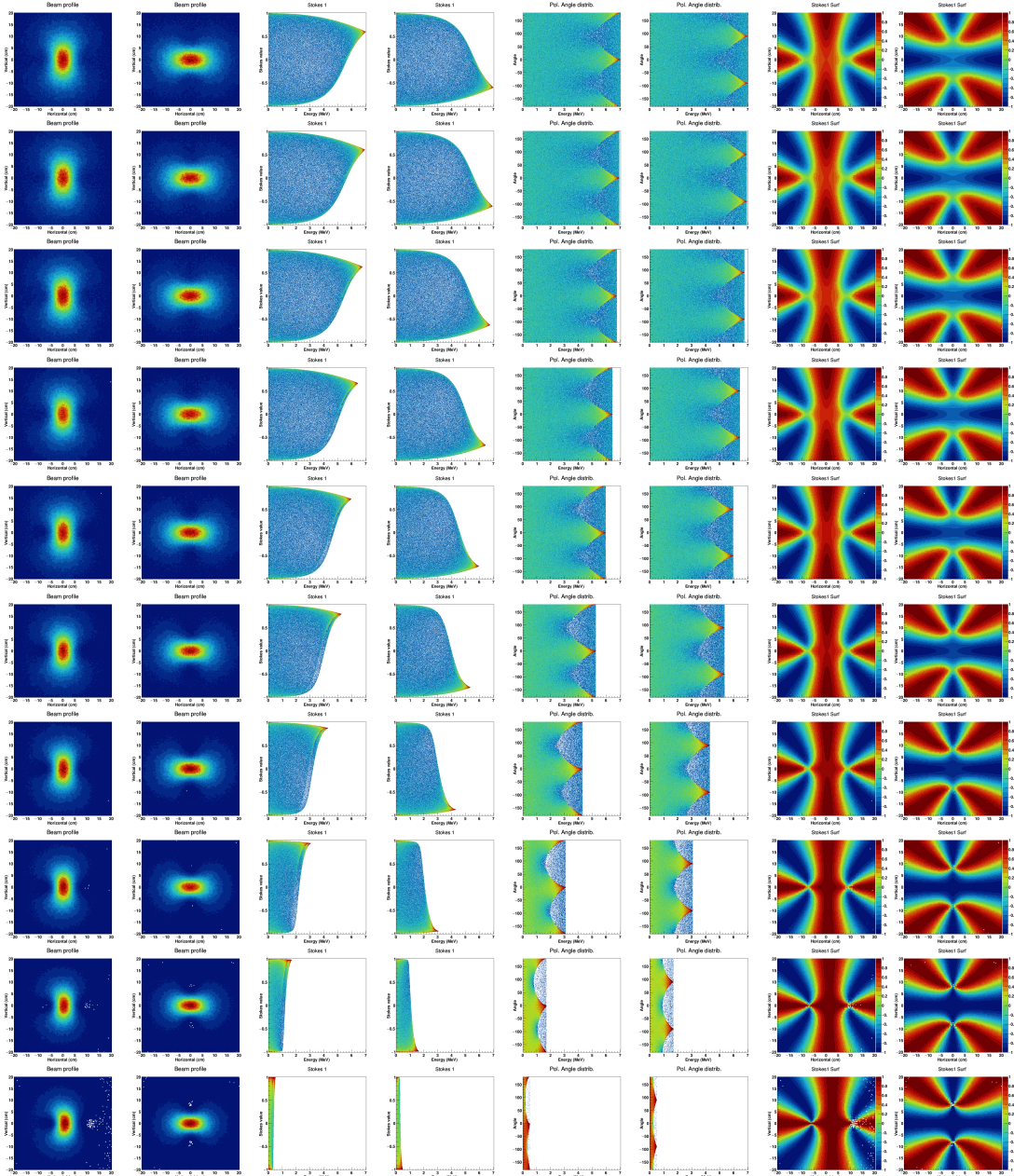


Figure 2. Compton scattering of 100 % linear polarized 100 pm wavelength X-rays on 10 MeV electrons.

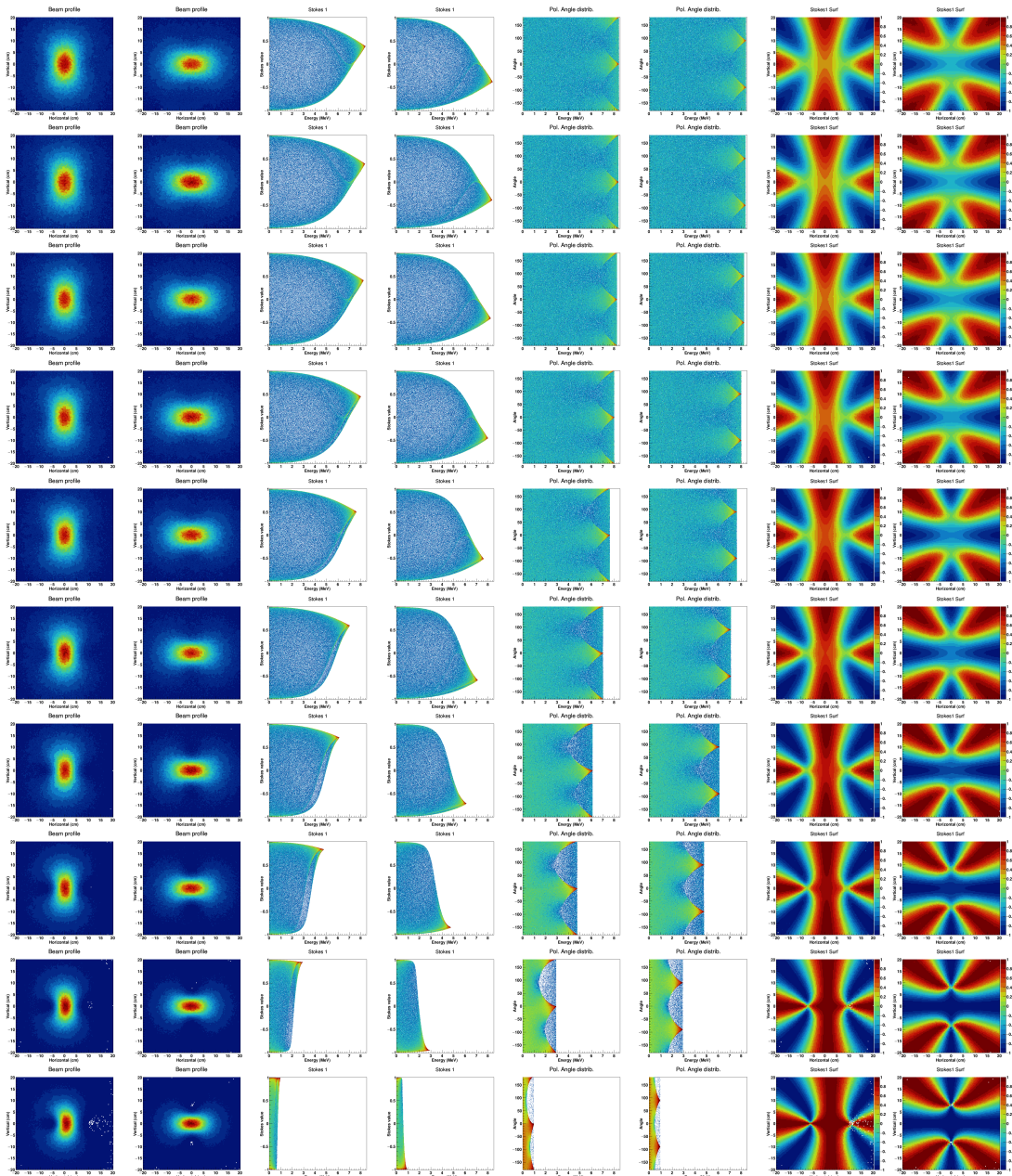


Figure 3. Compton scattering of 100 % linear polarized 50 pm wavelength X-rays on 10 MeV electrons.

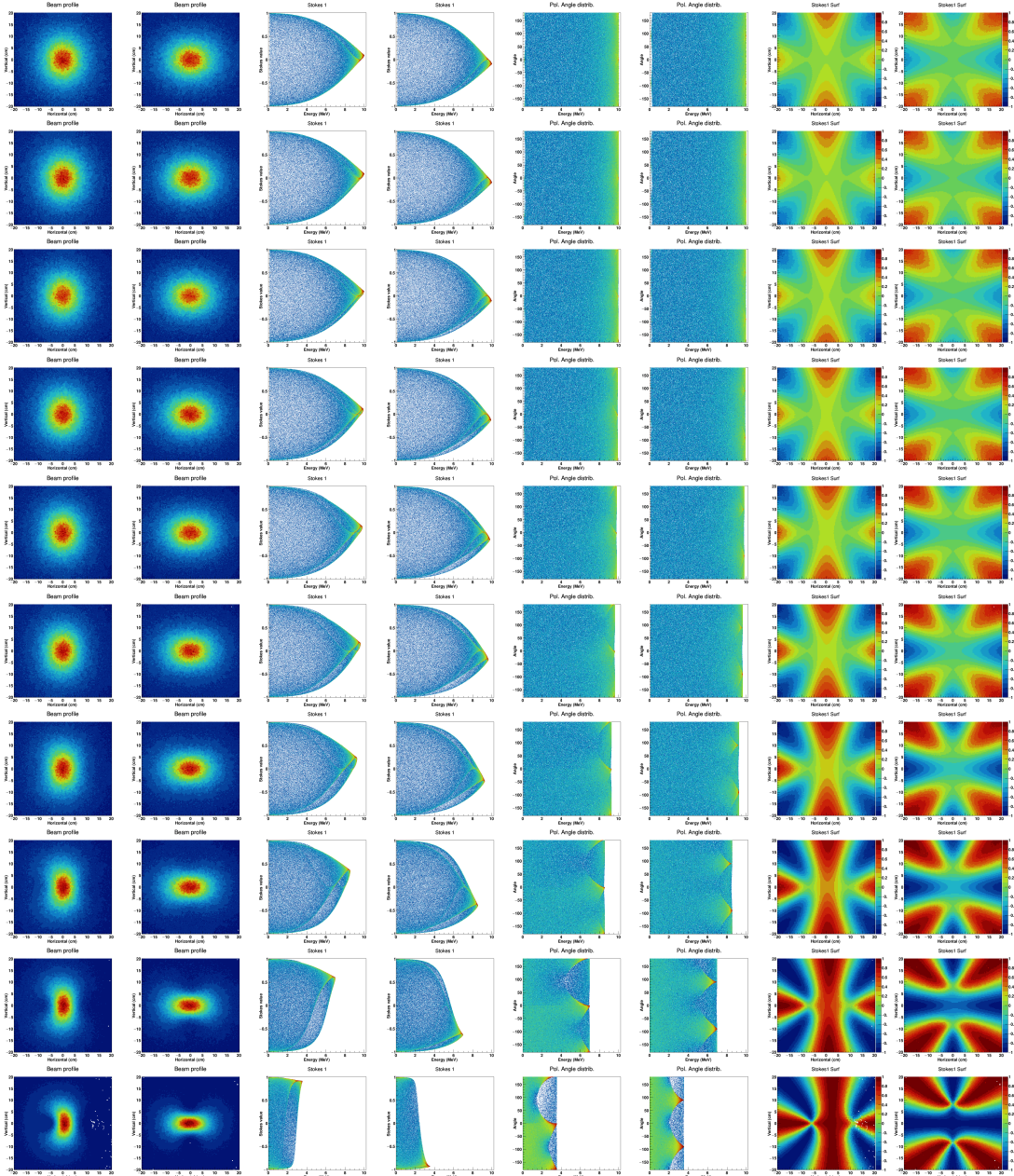


Figure 4. Compton scattering of 100 % linear polarized 10 pm wavelength X-rays on 10 MeV electrons.

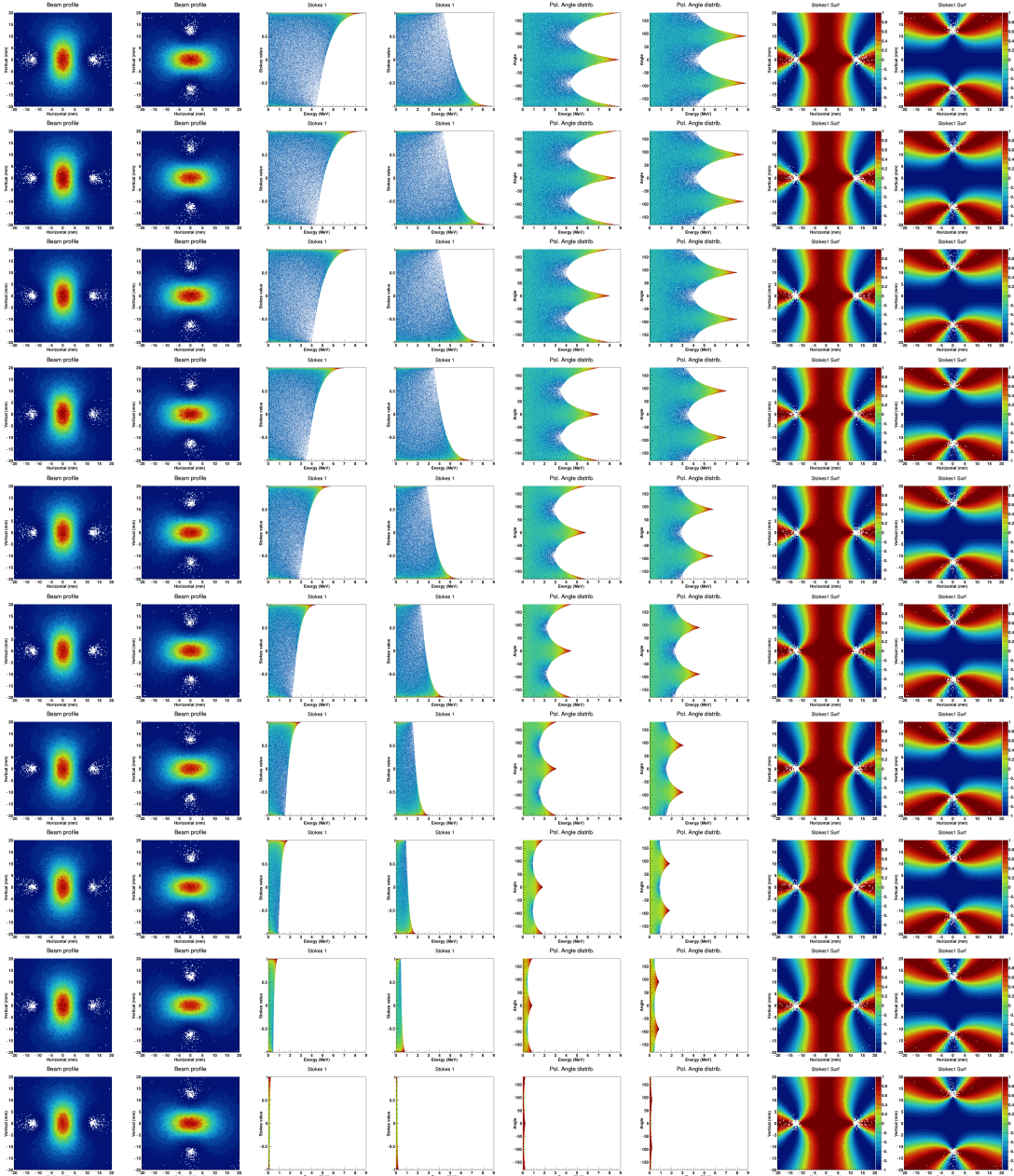


Figure 5. Compton scattering of 100 % linear polarized 532 nm wavelength laser on 500 MeV electrons.

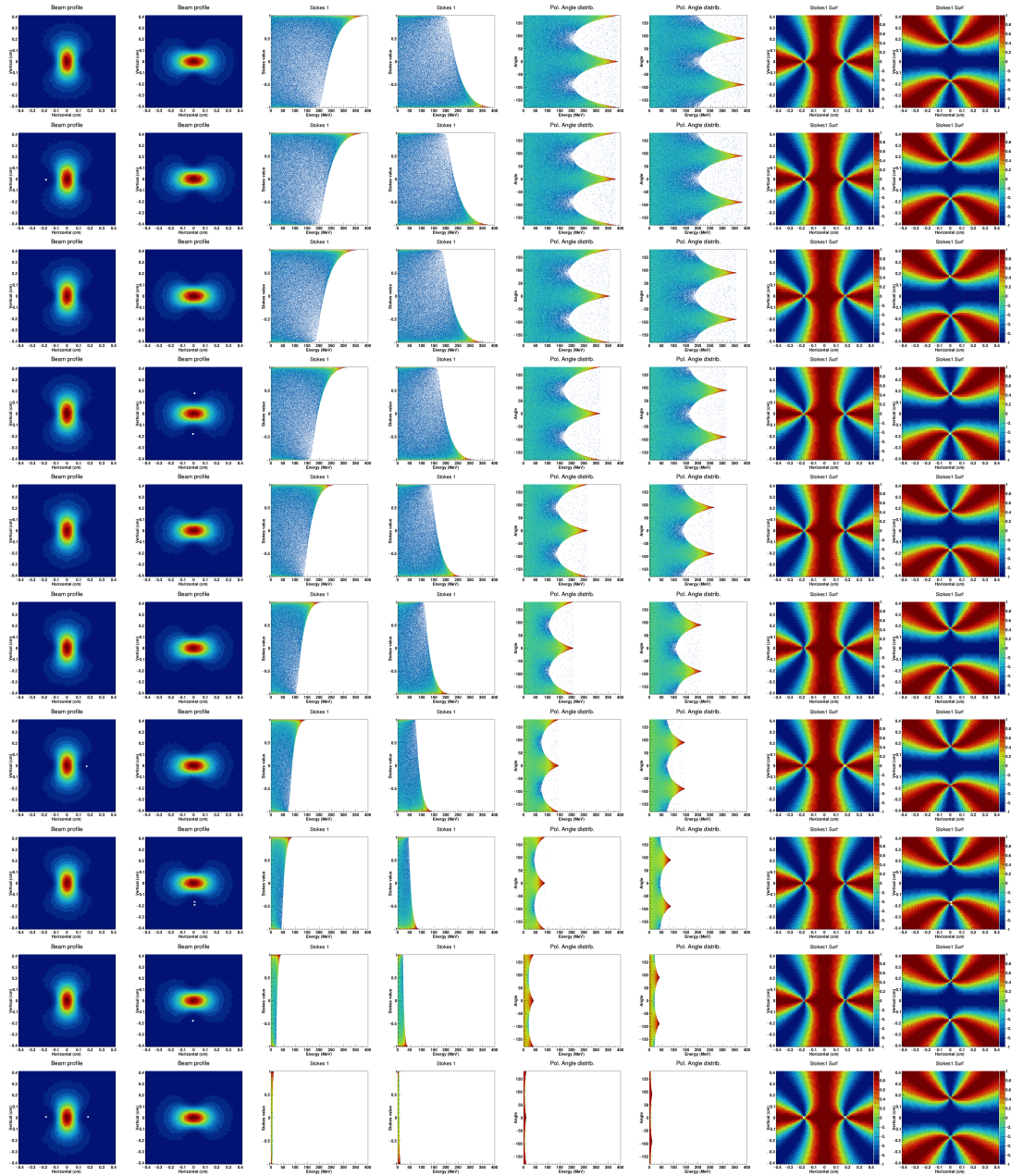


Figure 6. Compton scattering of 100 % linear polarized 532 nm wavelength laser on 3500 MeV electrons.